Reconfiguration analysis of a 3-DOF parallel mechanism using Euler parameter quaternions and algebraic geometry method

Kong, Xianwen

Published in:
Mechanism and Machine Theory

DOI:
10.1016/j.mechmachtheory.2013.12.010

Publication date:
2014

Mechanism and Machine Theory 74 (2014) 188–201

Contents lists available at ScienceDirect

Mechanism and Machine Theory

journal homepage: www.elsevier.com/locate/mechmt

Reconfiguration analysis of a 3-DOF parallel mechanism using Euler parameter quaternions and algebraic geometry method ☆

Xianwen Kong *

School of Engineering and Physical Sciences, Heriot-Watt University, Edinburgh EH14 4AS, UK

ARTICLE INFO

Article history:
Received 26 February 2013
Received in revised form 30 November 2013
Accepted 5 December 2013
Available online 28 December 2013

Keywords:
Parallel manipulator with multiple operation modes
Quaternion
Euler parameter
Singularity
Algebraic geometry

ABSTRACT

This paper deals with the reconfiguration analysis of a 3-DOF (degrees-of-freedom) parallel mechanism (PM) with multiple operation modes – a disassembly-free reconfigurable PM – using the Euler parameter quaternions and algebraic geometry approach. At first, Euler parameter quaternions are classified into 15 cases based on the number of constant zero components and the kinematic interpretation of different cases of Euler parameter quaternions is presented. A set of constraint equations of a 3-RER PM with orthogonal platforms is derived with the orientation of the moving platform represented using a Euler parameter quaternion and then solved using the algebraic geometry method. It is found that this 3-RER PM has 15 3-DOF operation modes, including four translational modes, six planar modes, four zero-torsion-rate motion modes and one spherical mode. The transition configurations, which are singular configurations, among different operation modes are also presented. Especially, the transition configurations in which the PM can switch among eight operation modes are revealed for the first time.

1. Introduction

Parallel mechanisms (PMs) with multiple operation modes [1,2] (also called PMs that change their group of motion [3], PMs with bifurcation of motion [4–6], or disassembly-free reconfigurable PMs [2]) are a novel class of reconfigurable PMs which need fewer actuators and less time for changeover than the existing reconfigurable PMs. Several classes of PMs with multiple operation modes have been proposed in the past decade.

A PM with multiple operation modes was first applied in a constant-velocity coupling to connect intersecting axes in one mode or parallel axes in another mode [7]. Since DYMO – a PM with multiple operation modes – was proposed in [8], several new PMs with multiple operation modes have been proposed [1–6,9]. How to switch a PM with multiple operation modes from one configuration to another requires reconfiguration analysis in order to fully understand all the operation modes that the PM has and the transition configurations between different operation modes. This requires solving polynomial equations with sets of positive dimensional solutions. Recent advances in algebraic geometry [10,11] and numerical algebraic geometry [12] as well as computer algebra systems [13] provide effective tools to the reconfiguration analysis.

This paper aims to fully investigate the operation modes of a 3-RER PM and the transition configurations to switch from one operation mode to another. Here, R and E denote revolute and planar joints respectively. In Section 2, Euler parameter quaternions will be classified based on the number of constant zero components. The kinematic interpretation of different cases of Euler parameter quaternions will be discussed. In Section 3, the description of a 3-RER PM with orthogonal platforms will be presented. In Section 4, by representing the position and orientation of the moving platform using the Cartesian coordinates of a

* Tel.: +44 1314513688.
E-mail address: X.Kong@hw.ac.uk.

0094-114X/$ – see front matter © 2013 The Author. Published by Elsevier Ltd. All rights reserved.
http://dx.doi.org/10.1016/j.mechmachtheory.2013.12.010

point on the moving platform and a Euler parameter quaternion respectively, a set of kinematic equations of the 3-RER PM will be derived and then solved using the algebraic geometry method to obtain all the operation modes of the PM. The transition configurations among different operation modes will be obtained in Section 5. Finally, conclusions will be drawn.

2. Classification of Euler parameter quaternions

Euler parameter quaternions, which are more computationally efficient than the transformation matrices, have been used in kinematics, computer visualization and animation, and aircraft navigation [14,15]. In this section, we will first recall the definition and operation of the Euler parameter quaternions and then discuss the classification and kinematic interpretation of the Euler parameter quaternions.

The Euler parameter quaternion is defined as (Fig. 1)

$$q = e_0 + e_1\mathbf{i} + e_2\mathbf{j} + e_3\mathbf{k} = cos(\theta/2) + \mathbf{u}sin(\theta/2) \tag{1}$$

where $\mathbf{u}$ and θ represent respectively the axis[1] and angle of rotation. The Euler parameters satisfy

$$e_0^2 + e_1^2 + e_2^2 + e_3^2 = 1. \tag{2}$$

Let $q = e_0 + e_1\mathbf{i} + e_2\mathbf{j} + e_3\mathbf{k}$, the conjugate of q is

$$q^* = e_0 - e_1\mathbf{i} - e_2\mathbf{j} - e_3\mathbf{k}. \tag{3}$$

The product of two Euler parameter quaternions satisfies the following rules:

$$\begin{aligned} &\mathbf{i}^2 = \mathbf{j}^2 = \mathbf{k}^2 = \mathbf{ijk} = -1\\ &\mathbf{ij} = \mathbf{k} = -\mathbf{ji}\\ &\mathbf{jk} = \mathbf{i} = -\mathbf{kj}\\ &\mathbf{ki} = \mathbf{j} = -\mathbf{ik}. \end{aligned} \tag{4}$$

A vector $\mathrm{r} = \{r_x r_y r_z\}^T$ can be written in quaternion form as $\mathbf{r} = r_x\mathbf{i} + r_y\mathbf{j} + r_z\mathbf{k}$. Let $\mathbf{r}' = r_x'\mathbf{i} + r_y'\mathbf{j} + r_z'\mathbf{k}$ denotes the vector obtained from a vector $\mathbf{r} = r_x\mathbf{i} + r_y\mathbf{j} + r_z\mathbf{k}$ by rotating it about the axis $\mathbf{u}$ by θ. We have

$$\mathbf{r}' = q\mathbf{r}q^*. \tag{5}$$

The compositional rotation composed of rotation q_1 followed by rotation q_2 can be represented using the following quaternion

$$q = q_2 q_1. \tag{6}$$

From Eq. (2), one learns that e_0, e_1, e_2 and e_3 cannot be equal to zero simultaneously. Euler parameter quaternions can then be classified into the following 15 cases according to the number of their constant 0 components:

$$\begin{aligned} &\{e_0, 0, 0, 0\}, \{0, e_1, 0, 0\}, \{0, 0, e_2, 0\}, \{0, 0, 0, e_3\}, \{e_0, e_1, 0, 0\}, \{e_0, 0, e_2, 0\},\\ &\{e_0, 0, 0, e_3\}, \{0, 0, e_2, e_3\}, \{0, e_1, 0, e_3\}, \{0, e_1, e_2, 0\}, \{0, e_1, e_2, e_3\}, \{e_0, 0, e_2, e_3\}\\ &\{e_0, e_1, 0, e_3\}, \{e_0, e_1, e_2, 0\} \text{ and } \{e_0, e_1, e_2, e_3\}. \end{aligned}$$

Using Eq. (1), we can identify the kinematic meaning of nine cases of Euler parameter quaternions (Nos. 1–7, 11 and 15 in Table 1) directly. For example, the Euler parameter quaternion of case {0, e_1, 0, 0} is $q = \mathbf{i}$ (No. 2 in Table 1), which represents a half-turn rotation about the X-axis. The DOF of the above motion is 0 and the angular velocity is 0. The Euler parameter quaternion of case {e_0, e_1, 0, 0} is $q = e_0 + e_1\mathbf{i}$ (No. 2 in Table 1), which represents a rotation by $2atan(e_1, e_0)$ about the X-axis. The DOF of the above motion is 1 and the axis of the angular velocity is the X-axis. The Euler parameter quaternion of case {0, e_1, e_2, e_3} is $q = e_1\mathbf{i} + e_2\mathbf{j} + e_3\mathbf{k}$ (No. 11 in Table 1). Kinematically, it refers to a half-turn rotation about the axis $\mathbf{u} = \{e_1\ e_2\ e_3\}^T$. Since the angle of rotation about the axis $\mathbf{u} = \{e_1\ e_2\ e_3\}^T$ is a constant, the component of the angular velocity along this axis is zero. The above motion can therefore be called a 2-DOF zero-torsion-rate rotation. It is noted that such a rotation is called a zero-torsion rotation in [16]. However, the torsion angle under the above motion is a constant and may not be zero depending on the mathematical representation of rotation.

For the remaining six cases of Euler parameter quaternions (Nos. 8–10 and 12–14 in Table 1), we cannot obtain explicitly the axis of angular velocity for a 1-DOF rotation and the axis along which the component of the angular velocity is zero for a 2-DOF rotation by using Eq. (1) directly. By factoring each of these six cases of Euler parameter quaternions as the product of two cases of Euler parameter quaternions (Nos. 1–7 and 11 in Table 1), one can identify their kinematic interpretation which reflects the motion characteristics using Eqs. (1) and (6).

[1] Throughout this paper, the axis $\mathbf{u}$ passes through the origin O of the reference coordinate system O-XYZ of a mechanism.

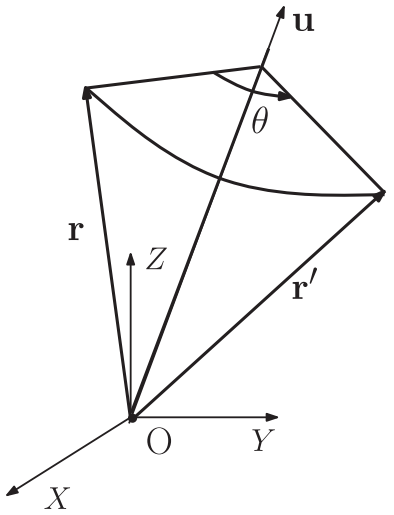

Fig. 1. Rotation by *theta* about axis u.

The rotation associated with a Euler parameter quaternion with two constant 0 components including a zero first component (Nos. 8–10 in Table 1) is a 1-DOF rotation. In order to reflect explicitly the axis of angular velocity, the Euler parameter quaternion should be decomposed as the product of a unit quaternion with two constant 0 components and a non-zero first component (Nos. 5–7 in Table 1) and a constant quaternion (see Nos. 2–4 in Table 1). For example, the Euler parameter quaternion of case {0, 0, e_2, e_3} is $q = e_2\mathbf{j} + e_3\mathbf{k}$. Although the quaternion can be interpreted as half-turn rotation about the axis $\mathbf{u} = \{0\ e_2\ e_3\}^T$ using Eq. (1), the axis of angular velocity is not indicated explicitly. To better reflect the motion characteristics of this quaternion, q is factored as

$$q = e_2\mathbf{j} + e_3\mathbf{k} = (e_2 + e_3\mathbf{i})\mathbf{j}. \tag{7}$$

Equation (7) shows that $q = e_2\mathbf{j} + e_3\mathbf{k}$ represents kinematically a half-turn rotation about the *Y*-axis followed by a rotation by $2atan(e_3, e_2)$ about the *X*-axis. The axis of the angular velocity associated with q is the *X*-axis.

Table 1
Classification of Euler parameter quaternions and their kinematic interpretation.

No	Case	Euler parametric quaternion	DOF	Motion description
1	$\{e_0, 0, 0, 0\}$	$q = 1$	0	No rotation
2	$\{0, e_1, 0, 0\}$	$q = \mathbf{i}$		Half-turn rotation about the *X*-axis
3	$\{0, 0, e_2, 0\}$	$q = \mathbf{j}$		Half-turn rotation about the *Y*-axis
4	$\{0, 0, 0, e_3\}$	$q = \mathbf{k}$		Half-turn rotation about the *Z*-axis
5	$\{e_0, e_1, 0, 0\}$	$q = e_0 + e_1\mathbf{i}$	1	Rotation by $2atan\ (e_1, e_0)$ about the *X*-axis
6	$\{e_0, 0, e_2, 0\}$	$q = e_0 + e_2\mathbf{j}$		Rotation by $2atan(e_2, e_0)$ about the *Y*-axis
7	$\{e_0, 0, 0, e_3\}$	$q = e_0 + e_3\mathbf{k}$		Rotation by $2atan(e_3, e_0)$ about the *Z*-axis
8	$\{0, 0, e_2, e_3\}$	$q = e_2\mathbf{j} + e_3\mathbf{k} = (e_2 + e_3\mathbf{i})\mathbf{j}$		Half-turn rotation about the *Y*-axis followed by a rotation by $2atan(e_3, e_2)$ about the *X*-axis
		$q = e_2\mathbf{j} + e_3\mathbf{k} = (e_3 - e_2\mathbf{i})\mathbf{k}$		Half-turn rotation about the *Z*-axis followed by a rotation by $2atan(-e_2, e_3)$ about the *X*-axis
9	$\{0, e_1, 0, e_3\}$	$q = e_1\mathbf{i} + e_3\mathbf{k} = (e_1 - e_3\mathbf{j})\mathbf{i}$		Half-turn rotation about the *X*-axis followed by a rotation by $2atan(-e_3, e_1)$ about the *Y*-axis
		$q = e_1\mathbf{i} + e_3\mathbf{k} = (e_3 + e_1\mathbf{j})\mathbf{k}$		Half-turn rotation about the *Z*-axis followed by a rotation by $2atan(e_1, e_3)$ about the *Y*-axis
10	$\{0, e_1, e_2, 0\}$	$q = e_1\mathbf{i} + e_2\mathbf{j} = (e_1 + e_2\mathbf{k})\mathbf{i}$		Half-turn rotation about the *X*-axis followed by a rotation by $2atan(e_2, e_1)$ about the *Z*-axis
		$q = e_1\mathbf{i} + e_2\mathbf{j} = (e_2 - e_1\mathbf{k})\mathbf{j}$		Half-turn rotation about the *Y*-axis followed by a rotation by $2atan(-e_1, e_2)$ about the *Z*-axis
11	$\{0, e_1, e_2, e_3\}$	$q = e_1\mathbf{i} + e_2\mathbf{j} + e_3\mathbf{k}$	2	Half-turn rotation about the axis $\mathbf{u} = \{e_1\ e_2\ e_3\}^T$
12	$\{e_0, 0, e_2, e_3\}$	$q = e_0 + e_2\mathbf{j} + e_3\mathbf{k} = (-e_0\mathbf{i} - e_3\mathbf{j} + e_2\mathbf{k})\mathbf{i}$		Half-turn rotation about the *X*-axis followed by a half-turn rotation about the axis $\mathbf{u} = \{-e_0\ -e_3\ e_2\}^T$
13	$\{e_0, e_1, 0, e_3\}$	$q = e_0 + e_1\mathbf{i} + e_3\mathbf{k} = (e_3\mathbf{i} - e_0\mathbf{j} - e_1\mathbf{k})\mathbf{j}$		Half-turn rotation about the *Y*-axis followed by a half-turn rotation about the axis $\mathbf{u} = \{e_3\ -e_0\ -e_1\}^T$
14	$\{e_0, e_1, e_2, 0\}$	$q = e_0 + e_1\mathbf{i} + e_2\mathbf{j} = (-e_2\mathbf{i} + e_1\mathbf{j} - e_0\mathbf{k})\mathbf{k}$		Half-turn rotation about the *Z*-axis followed by a half-turn rotation about the axis $\mathbf{u} = \{-e_2\ e_1\ -e_0\}^T$
15	$\{e_0, e_1, e_2, e_3\}$	$q = e_0 + e_1\mathbf{i} + e_2\mathbf{j} + e_3\mathbf{k}$	3	Spherical motion

The rotation associated with a Euler parameter quaternion with one constant 0 component which is not the first component (Nos. 12–14 in Table 1) is a 2-DOF rotation. In order to reflect explicitly the axis along which the component of the angular velocity is zero, the Euler parameter quaternion should be decomposed as the product of a unit quaternion with a constant 0 component which is the first component (No. 11 in Table 1) and a constant quaternion (see Nos. 2–4 in Table 1). For example, the Euler parameter quaternion of case $\{e_0, 0, e_2, e_3\}$ is $q = e_0 + e_2\mathbf{j} + e_3\mathbf{k}$. Although the quaternion can be interpreted as a rotation about the axis $\mathbf{u} = \{0\ e_2\ e_3\}^T$ using Eq. (1), the axis along which the component of the angular velocity is zero is not indicated explicitly. To better reflect the motion characteristics of this quaternion, q is factored as

$$q = (-e_0\mathbf{i} - e_3\mathbf{j} + e_2\mathbf{k})\mathbf{i}. \tag{8}$$

Eq. (8) shows that $q = e_0 + e_2\mathbf{j} + e_3\mathbf{k}$ represents kinematically a half-turn rotation about the X-axis followed by a half-turn rotation about the axis $\mathbf{u} = \{-e_0\ -e_3\ e_2\}^T$. The component of the angular velocity associated with q along the axis $\mathbf{u} = \{-e_0\ -e_3\ e_2\}^T$ is zero.

The kinematic interpretation of all the 15 cases of Euler parameter quaternions is given in Table 1.

As it will be shown in Section 4, each case of Euler parameter quaternions is associated with one operation mode of the 3-RER PM studied in this paper.

3. Description of a 3-DOF 3-RER PM with orthogonal platforms

A 3-DOF 3-RER PM with orthogonal platforms (Fig. 2) is composed of a moving platform connected to the base by three RER legs. The axes of the three R joints on the moving platform (base) are orthogonal and have a common point. Each leg is a serial kinematic chain composed of R, E and R joints in sequence in such a way that the axes of these two R joints are always coplanar. An E joint can be any planar kinematic chain such as RRR (Fig. 2) and RPR kinematic chains. Here P denotes a prismatic joint. Fig. 3 shows a configuration of the RER leg in which the structure characteristics of the leg can be easily observed: the axes of R joints 1 and 5 are collinear, the axes of the remaining three R joints within the E joint are perpendicular to the axes of R joints 1 and 5 (Fig. 3(a) and (b)). The special RER leg also satisfies the following conditions: Two pairs of R joints, joints 1 and 2 as well as joints 4 and 5, have perpendicular and intersecting joint axes, and links 2 and 3 have equal link lengths (Fig. 3(b)). In addition, the axis of joint 2(4) of each special RER leg in the 3-RER PM passes through the intersection of the joint axes of three R joints on the base (moving platform). As it will be shown later, the introduction of the special RER leg (Fig. 3(b)) facilitates the reconfiguration of the 3-RER PM from one operation mode to another manually and does not affect the operation modes of the moving platform. Links 1 and 4 in each leg are curved in order to avoid link interference during reconfiguration.

Let O–XYZ and O_p–$X_pY_pZ_p$ denote the coordinate frames fixed on the base and the moving platform respectively. The X-, Y- and Z-axes are, respectively, along the axes of the three R joints on the base. The X_p-, Y_p- and Z_p-axes are, respectively, along the axes of the three R joints on the moving platform. The X- and X_p-axes, Y- and Y_p-axes and Z- and Z_p-axes are connected by legs 1, 2 and 3 respectively.

Let $\mathbf{v}_i$ and $\mathbf{w}_i$ denote the unit vectors along the axes of the bottom and top R joints of leg i in the coordinate system O–XYZ and $\mathbf{w}_{Pi}$ denote the unit vector along the top R joint of leg i in the coordinate system O_p–$X_pY_pZ_p$. We have

$$\mathbf{v}_1 = \{1\ 0\ 0\}^T,\ \mathbf{v}_2 = \{0\ 1\ 0\}^T,\ \mathbf{v}_3 = \{0\ 0\ 1\}^T,\ \mathbf{w}_{P1} = \{1\ 0\ 0\}^T,\ \mathbf{w}_{P2} = \{0\ 1\ 0\}^T \quad \text{and} \quad \mathbf{w}_{P3} = \{0\ 0\ 1\}^T.$$

In the reference configuration, the coordinate systems O_p–$X_pY_pZ_p$ and O–XYZ coincide with each other. Let the location of the coordinate system O_p–$X_pY_pZ_p$ in the coordinate system O–XYZ be represented by the position of O_p, denoted by

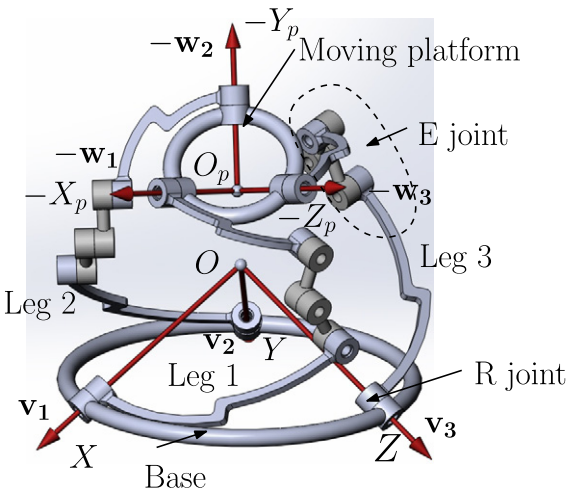

Fig. 2. 3-RER PM with orthogonal platforms.

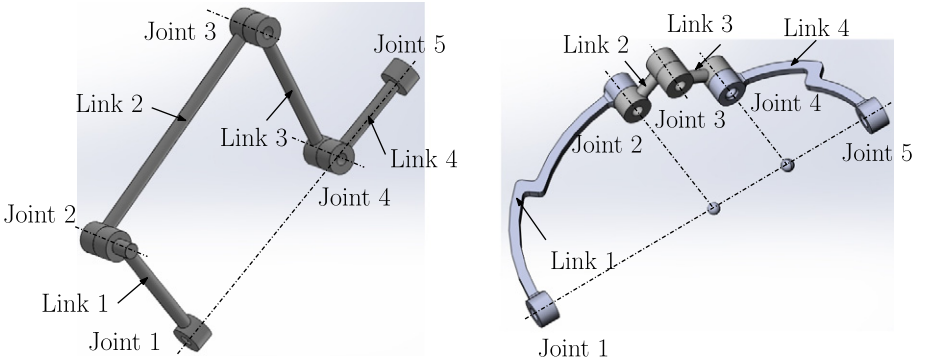

(a) General case. (b) Special case.

Fig. 3. RER leg.

$\mathbf{O}_p = \{x\, y\, z\}^T$, and the orientation of the moving platform, denoted by the Euler parameter quaternion q (see Eq. (1)). From Eq. (5), we obtain

$$\begin{cases} \mathbf{w}_1 = q\mathbf{i}q^* \\ \mathbf{w}_2 = q\mathbf{j}q^* \\ \mathbf{w}_3 = q\mathbf{k}q^*. \end{cases} \tag{9}$$

Substituting Eqs. (1) and (4) into Eq. (9), we have

$$\begin{cases} \mathbf{w}_1 = \left(e_0^2 + e_1^2 - e_2^2 - e_3^2\right)\mathbf{i} + 2(e_1e_2 + e_0e_3)\mathbf{j} + 2(e_1e_3 - e_0e_2)\mathbf{k} \\ \mathbf{w}_2 = 2(e_1e_2 - e_0e_3)\mathbf{i} + \left(e_0^2 - e_1^2 + e_2^2 - e_3^2\right)\mathbf{j} + 2(e_2e_3 + e_0e_1)\mathbf{k} \\ \mathbf{w}_3 = 2(e_1e_3 + e_0e_2)\mathbf{i} + 2(e_2e_3 - e_0e_1)\mathbf{j} + \left(e_0^2 - e_1^2 - e_2^2 + e_3^2\right)\mathbf{k}. \end{cases}$$

Rewriting the above equation in the Cartesian vector form, we have

$$\begin{cases} \mathbf{w}_1 = \left\{e_0^2 + e_1^2 - e_2^2 - e_3^2 2(e_1e_2 + e_0e_3) 2(e_1e_3 - e_0e_2)\right\}^T \\ \mathbf{w}_2 = \left\{2(e_1e_2 - e_0e_3) e_0^2 - e_1^2 + e_2^2 - e_3^2 2(e_2e_3 + e_0e_1)\right\}^T \\ \mathbf{w}_3 = \left\{2(e_1e_3 + e_0e_2) 2(e_2e_3 - e_0e_1) e_0^2 - e_1^2 - e_2^2 + e_3^2\right\}^T. \end{cases} \tag{10}$$

In each RER leg, the axes of the two R joints are always coplanar due to the constraint imposed by the E joint, i.e., the triple product of the two unit vectors along the axes of the bottom and top R joints of leg i and vector $\mathbf{O}_p$ is equal to zero. The set of constraint equations of leg i ($i = 1$, 2 and 3) is then obtained as

$$\mathbf{w}_i \times \mathbf{v}_\mathbf{i} \cdot \mathbf{O}_p = 0.$$

Expanding the above equation in scalar form, we have

$$\begin{cases} -e_1e_3y + e_0e_2y + e_1e_2z + e_0e_3z = 0 \\ e_2e_3x + e_0e_1x - e_1e_2z + e_0e_3z = 0 \\ -e_2e_3x + e_0e_1x + e_1e_3y + e_0e_2y = 0. \end{cases} \tag{11}$$

Eqs. (11) and (2) are the equations for the reconfiguration analysis of the 3-RER PM.

4. Operation modes analysis of the 3-RER PM with orthogonal platforms

In the type synthesis of PMs with multiple operation modes [1,2,3,4,5,6], a PM with multiple operation modes is obtained in a transition configuration that the PM can transit between two operation modes. Therefore, there must be at least two sets of positive dimension solutions, each corresponding to one operation mode, to the set of constraint equations of the PM. In order to reconfigure the PM, one needs to fully understand all the operation modes and the transition configurations of the PM. The methods based on algebraic geometry [10,11] or numerical algebraic geometry [12] as well as computer algebra systems [13]

provide effective tools to find all the sets of positive dimension solutions to a set of constraint (polynomial) equations and to solve the above reconfiguration analysis problem.

The operation mode analysis of the 3-RER PM can be carried out by the prime decomposition of the ideal associated with the set of constraint equations (Eq. (11)) for the 3-RER PM. All the operation modes satisfy Eq. (2), which will be omitted in the representation of operation modes and transition configurations of the 3-RER PM for brevity reasons.

The ideal associated with Eq. (11) for the 3-RER PM with orthogonal base and platform is

$$\mathcal{I} = <-e_1e_3y + e_0e_2y + e_1e_2z + e_0e_3z, e_2e_3x + e_0e_1x - e_1e_2z + e_0e_3z, -e_2e_3x + e_0e_1x + e_1e_3y + e_0e_2y>.$$

Since this ideal is rather simple, we can obtain its prime decomposition directly using the software SINGULAR [13] as follows:

$$\mathcal{I} = \bigcap_{j=1}^{15} \mathcal{I}_j \tag{12}$$

where

$$\mathcal{I}_1 = <e_1, e_2, e_3>, \mathcal{I}_2 = <e_0, e_2, e_3>, \mathcal{I}_3 = <e_0, e_1, e_3>, \mathcal{I}_4 = <e_0, e_1, e_2>,$$
$$\mathcal{I}_5 = <e_2, e_3, x>, \mathcal{I}_6 = <e_0, e_1, x>, \mathcal{I}_7 = <e_1, e_3, y>, \mathcal{I}_8 = <e_0, e_2, y>,$$
$$\mathcal{I}_9 = <e_1, e_2, z>, \mathcal{I}_{10} = <e_0, e_3, z>, \mathcal{I}_{11} = <e_0, -e_3y + e_2z, -e_3x + e_1z, -e_2x + e_1y>$$
$$\mathcal{I}_{12} = <e_1, e_2y + e_3z, e_2x + e_0z, -e_3x + e_0y>, \mathcal{I}_{13} = <e_2, e_1x + e_3z, -e_1y + e_0z, e_0x + e_3y>$$
$$\mathcal{I}_{14} = <e_3, e_1x + e_2y, e_0y + e_1z, e_0x - e_2z> \text{ and } \mathcal{I}_{15} = <x, y, z>.$$

Then, we can obtain 15 sets of positive-dimension solutions, each corresponding to one operation mode, that satisfy both Eqs. (11) and (2). These 15 sets of positive-dimension solutions are listed in the third column in Table 2.

With the aid of the classification and kinematic interpretation of Euler parameter quaternions (Table 1), we can reveal the motion characteristics in each operation mode of the 3-RER PM with orthogonal platforms.

Let us take the No. 11 operation mode in Table 2 as an example. The set of constraint equations of the No. 11 operation mode is

$$\begin{cases} e_0 = 0 \\ -e_3y + e_2z = 0 \\ -e_3x + e_1z = 0 \\ -e_2x + e_1y = 0. \end{cases} \tag{13}$$

It is apparent that the first equation in Eq. (13) is in fact Case 11 of the Euler parameter quaternions. This means that the moving platform will undergo a half-turn rotation about the axis $\mathbf{u} = \{e_1\ e_2\ e_3\}^T$. The last three equations in Eq. (13) is in fact $\mathbf{O_p} \times \mathbf{u} = 0$, which means that the moving platform can translate along the direction $\mathbf{u}$. The motion in this mode is called a 3-DOF zero-torsion-rate motion considering that the component of angular velocity of the moving platform along $\mathbf{u}$ is zero. Figure 4 shows the prototype of a 3-RER PM fabricated at Heriot-Watt University in the No. 11 operation mode. Please note that the extra holes on the base and moving platform are used for assembling PM models other than the 3-RER PM with orthogonal platforms.

The above example shows that the classification and kinematic interpretation of Euler parameter quaternions provide an efficient way for revealing the motion characteristics of different operation modes of the 3-RER PM. Unlike the method presented in [11], there is no need to compute the rotation matrix and the associated eigenspace for each operation mode.

A description of motion of the moving platform in each of the 15 modes has been obtained and given in Table 2. Figs. 5–8 show the configurations, each in one of the 15 operation modes, of the 3-RER PM. Most of the motion described in Table 2 in each operation mode can be verified readily using the results in the literature. In operation modes Nos. 1–4 (Fig. 5(a) and (b)), the axes of joints 1 and 5 in each leg are parallel to each other, and axes of joints 2–4 in each leg are parallel. The PM in these operation modes satisfies the conditions for translational PMs [1]. Therefore, the moving platform undergoes 3-DOF spatial translation. In operation modes Nos. 5–10 (Fig. 6(a) and (b)), the axes of joints 1 and 5 in one leg are parallel to the axes of joints 2, 3 and 4 in the other two legs. Since the PM in these operation modes satisfies the conditions for planar PMs [2], the moving platform undergoes 3-DOF planar motion. In operation mode No. 15 (Fig. 8), the axes of joints 1, 2, 4 and 5 in all the three legs have a common point for the PM with the special legs, and the axes of joints 1 and 5 in all the three legs have a common point while the axes of joints 2, 3 and 4 in each leg are parallel for the PM with three general legs. The moving platform can thus undergo 3-DOF spherical motion [1].

It is noted that in the 3-RER PM with the special legs (Fig. 8), the axes of joints 2 and 4 in each leg coincide in operation mode No. 15. Links 2 and 3 in each leg can rotate freely about the axes of joints 2 and 4 within the same leg. The total DOF of the PM in operation mode No. 15 is 6 although the moving platform has 3 DOFs.

5. Transition configuration analysis

Transition configuration analysis is an important issue in the design and control of PMs with multiple operation modes. To find the transition configurations among n_m operation modes is to solve the set of constraint equations composed of the n_m sets of constraint equations associated with these operation modes. Due to space limitation, the transition configurations for cases $n_m = 2$ and $n_m = 8$ will be presented in this section.

Table 2
Fifteen operation modes of the 3-RER PM with orthogonal platforms.

No	Class	Constraint equations	Description
1	3-DOF spatial translation	$\begin{cases} e_1 = 0 \\ e_2 = 0 \\ e_3 = 0 \end{cases}$	Spatial translation
2		$\begin{cases} e_0 = 0 \\ e_2 = 0 \\ e_3 = 0 \end{cases}$	Spatial translation following a half-turn rotation about the *X*-axis
3		$\begin{cases} e_0 = 0 \\ e_1 = 0 \\ e_3 = 0 \end{cases}$	Spatial translation following a half-turn rotation about the *Y*-axis
4		$\begin{cases} e_0 = 0 \\ e_1 = 0 \\ e_2 = 0 \end{cases}$	Spatial translation following a half-turn rotation about the *Z*-axis
5	3-DOF planar motion	$\begin{cases} e_2 = 0 \\ e_3 = 0 \\ x = 0 \end{cases}$	3-DOF planar motion along the *O–YZ* plane
6		$\begin{cases} e_0 = 0 \\ e_1 = 0 \\ x = 0 \end{cases}$	Planar motion along the *O–YZ* plane following a half-turn rotation about the *Y*-axis or *Z*-axis
7		$\begin{cases} e_1 = 0 \\ e_3 = 0 \\ y = 0 \end{cases}$	Planar motion along the *O–XZ* plane
8		$\begin{cases} e_0 = 0 \\ e_2 = 0 \\ y = 0 \end{cases}$	Planar motion along the *O–XZ* plane following a half-turn rotation about the *X*-axis or *Z*-axis
9		$\begin{cases} e_1 = 0 \\ e_2 = 0 \\ z = 0 \end{cases}$	Planar motion along the *O–XY* plane
10		$\begin{cases} e_0 = 0 \\ e_3 = 0 \\ z = 0 \end{cases}$	Planar motion along the *O–XY* plane following a half-turn rotation about the *X*-axis or *Y*-axis
11	3-DOF zero-torsion-rate motion	$\begin{cases} e_0 = 0 \\ -e_3 y + e_2 z = 0 \\ -e_3 x + e_1 z = 0 \\ -e_2 x + e_1 y = 0 \end{cases}$	Half-turn rotation about the axis $\mathbf{u} = \{e_1\ e_2\ e_3\}^T$ followed by a translation along the direction $\mathbf{u} = \{e_1\ e_2\ e_3\}^T$.
12		$\begin{cases} e_1 = 0 \\ e_2 y + e_3 z = 0 \\ e_2 x + e_0 z = 0 \\ -e_3 x + e_0 y = 0 \end{cases}$	Half-turn rotation about the *X*-axis followed by a half-turn rotation about the axis $\mathbf{u} = \{-e_0\ -e_3\ e_2\}^T$ and subsequent translation along the direction $\mathbf{u} = \{-e_0\ -e_3\ e_2\}^T$.
13		$\begin{cases} e_2 = 0 \\ e_1 x + e_3 z = 0 \\ -e_1 y + e_0 z = 0 \\ e_0 x + e_3 y = 0 \end{cases}$	Half-turn rotation about the *Y*-axis followed by a half-turn rotation about the axis $\mathbf{u} = \{e_3\ -e_0\ -e_1\}^T$ and subsequent translation along the direction $\mathbf{u} = \{e_3\ -e_0\ -e_1\}^T$.
14		$\begin{cases} e_3 = 0 \\ e_1 x + e_2 y = 0 \\ e_0 y + e_1 z = 0 \\ e_0 x - e_2 z = 0 \end{cases}$	Half-turn rotation about the *Z*-axis followed by a half-turn rotation about the axis $\mathbf{u} = \{-e_2\ e_1\ -e_0\}^T$ and subsequent translation along the direction $\mathbf{u} = \{-e_2\ e_1\ -e_0\}^T$.
15	3-DOF spherical motion	$\begin{cases} x = 0 \\ y = 0 \\ z = 0 \end{cases}$	Spherical motion

5.1. Case $n_m = 2$

To identify the transition configurations of the operation modes Nos. 11 and 15, T(11 ∧ 15), one needs to solve the following set of constraint equations, which is obtained by combining the two sets of constraint equations associated with these two operation modes (Table 2), as

$$\begin{cases} e_0 = 0 \\ -e_3 y + e_2 z = 0 \\ -e_3 x + e_1 z = 0 \\ -e_2 x + e_1 y = 0 \\ x = 0 \\ y = 0 \\ z = 0. \end{cases} \tag{14}$$

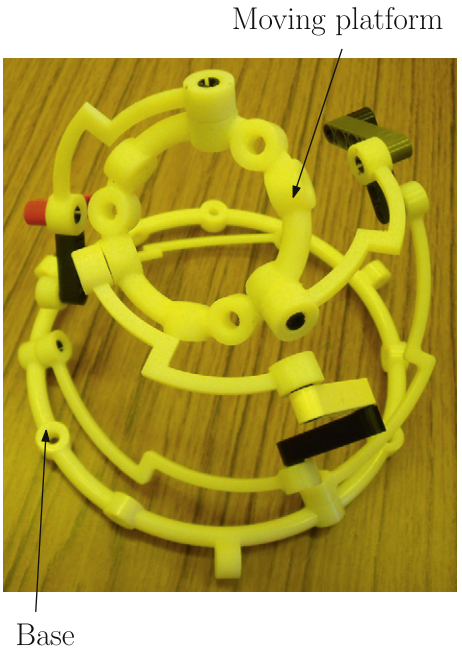

Fig. 4. A prototype of the 3-RER PM with orthogonal platforms in operation mode No. 11.

Simplifying Eq. (2), we obtain the transition configurations T(11 ∧ 15) as

$$\begin{cases} e_0 = 0 \\ x = 0 \\ y = 0 \\ z = 0. \end{cases} \tag{15}$$

The above equation represents all the configurations obtained through a 2-DOF zero-torsion-rate rotation about the axis $\mathbf{u} = \{e_1\ e_2\ e_3\}^T$.

All the transition configurations between two operation modes have been obtained. Due to space limitation, only those involving operation modes Nos. 1, 5, 11 and 15 are given since these operation modes are of different types of motion (Tables 3–6).

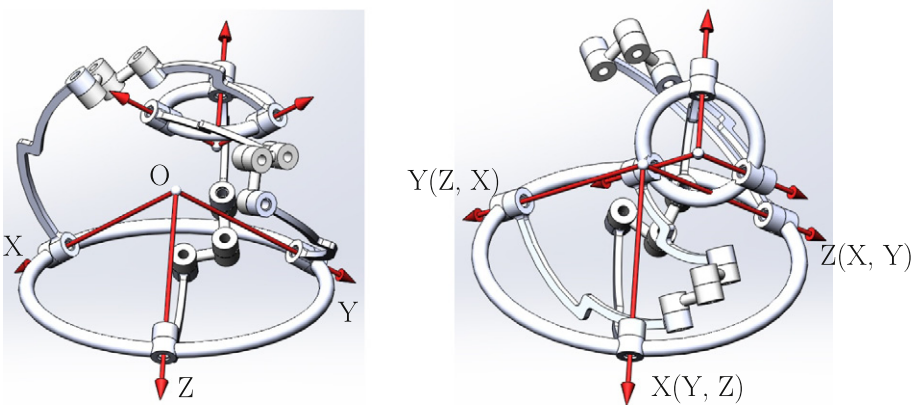

(a) Operation mode No. 1. (b) Operation mode No. 2(3 or 4).

Fig. 5. 3-RER parallel manipulator in four 3-DOF spatial translational motion modes: operation modes Nos. 1–4.

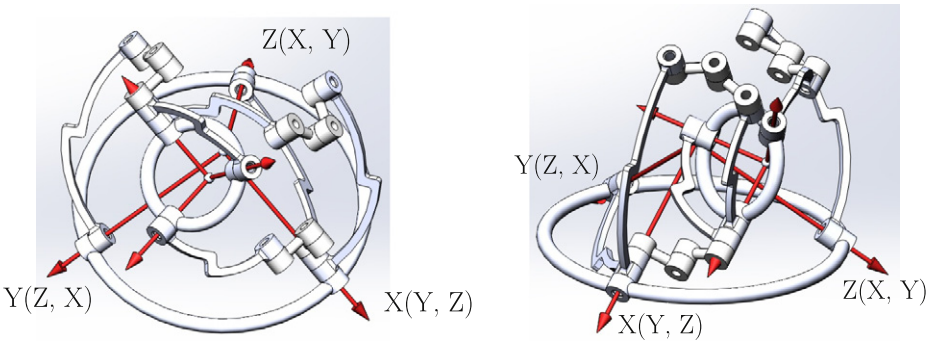

(a) Operation mode No. 5(7 or 9). (b) Operation mode No. 6(8 or 10).

Fig. 6. 3-RER parallel manipulator in six 3-DOF planar motion modes: operation modes Nos. 5–10.

It is noted from Table 6 that the 3-RER PM can switch between the 3-DOF spherical rotation mode (No. 15 operation mode) and any of the remaining 14 operation modes. By aligning the axes of joints 2 and 4 in each leg of the 3-RER PM (Fig. 8), one can easily switch the PM from any of the 14 operation modes, operation modes 1–14, to operational mode No. 15 (3-DOF spherical rotation mode) manually. It is not straightforward to switch the PM from an operation mode to operation mode No. 15 manually if a general RER leg (Fig. 3(a)) is used since it is not apparent when the axes of joints 1 and 5 in all the legs intersect at one point. That is why we use the special legs in the prototype of the 3-RER PM.

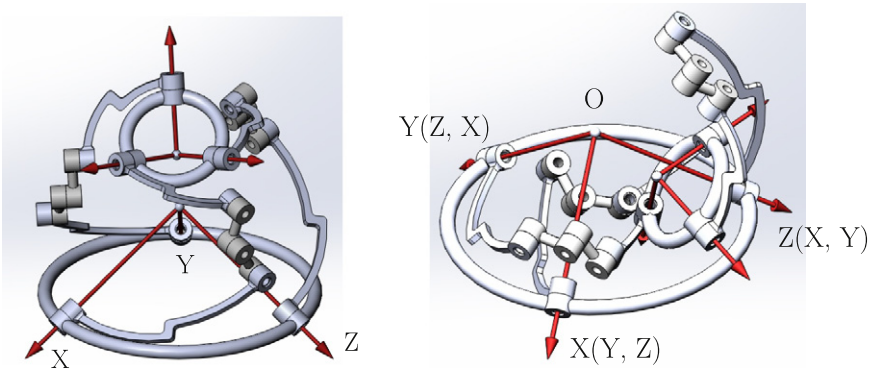

(a) Operation mode No. 11. (b) Operation mode No. 12(13 or 14).

Fig. 7. 3-RER parallel manipulator in four 3-DOF zero-torsion-rate motion modes: operation modes Nos. 11–14.

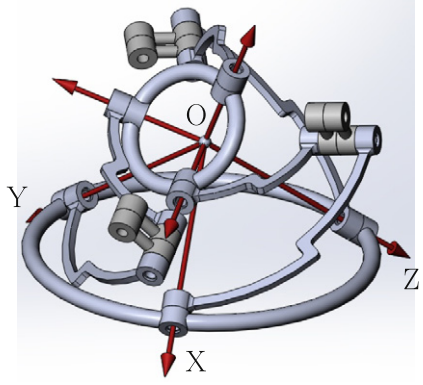

Fig. 8. 3-RER parallel manipulator in 3-DOF spherical motion mode: operation mode No. 15.

Table 3
Transition configurations between operation mode 1 and other operation modes T(1 ∧ *j*).

No	Constraint equations	Description
T(1 ∧ 2)	–	–
T(1 ∧ 3)	–	–
T(1 ∧ 4)	–	–
T(1 ∧ 5)	$\begin{cases} e_1 = 0 \\ e_2 = 0 \\ e_3 = 0 \\ x = 0 \end{cases}$	Configurations obtained through a translation along the *O–YZ* plane
T(1 ∧ 6)	–	–
T(1 ∧ 7)	$\begin{cases} e_1 = 0 \\ e_2 = 0 \\ e_3 = 0 \\ y = 0 \end{cases}$	Configurations obtained through a translation along the *O–XZ* plane
T(1 ∧ 8)	–	–
T(1 ∧ 9)	$\begin{cases} e_1 = 0 \\ e_2 = 0 \\ e_3 = 0 \\ z = 0 \end{cases}$	Configurations obtained through a translation along the *O–XY* plane
T(1 ∧ 10)	–	–
T(1 ∧ 11)	–	–
T(1 ∧ 12)	$\begin{cases} e_1 = 0 \\ e_2 = 0 \\ e_3 = 0 \\ y = 0 \\ z = 0 \end{cases}$	Configurations obtained through a translation along the *X*-axis
T(1 ∧ 13)	$\begin{cases} e_1 = 0 \\ e_2 = 0 \\ e_3 = 0 \\ x = 0 \\ z = 0 \end{cases}$	Configurations obtained through a translation along the *Y*-axis
T(1 ∧ 14)	$\begin{cases} e_1 = 0 \\ e_2 = 0 \\ e_3 = 0 \\ x = 0 \\ y = 0 \end{cases}$	Configurations obtained through a translation along the *Z*-axis
T(1 ∧ 15)	$\begin{cases} e_1 = 0 \\ e_2 = 0 \\ e_3 = 0 \\ x = 0 \\ y = 0 \\ z = 0 \end{cases}$	Reference configuration

5.2. Case $n_m = 8$

Starting from the transition configurations between two operation modes that we have obtained in Subsection 5.1, we can further find the transition configurations in which the 3-RER PM can switch among more than two operation modes.

From Table 3, we learn that the 3-RER PM can switch from operation mode No 1 to seven operation modes Nos. 5, 7, 9, 12, 13, 14 and 15 and cannot switch to the remaining seven operation modes. Then, we can find the transition configurations among n_m $(3 \le n_m \le 8)$ operation modes including operation mode No. 1. The transition configuration, T(1 ∧ 5 ∧ 7 ∧ 9 ∧ 12 ∧ 13 ∧ 14 ∧ 15), among the eight operation modes Nos. 1, 5, 7, 9, 12, 13, 14 and 15 that we obtained is

$$\begin{cases} e_1 = 0 \\ e_2 = 0 \\ e_3 = 0 \\ x = 0 \\ y = 0 \\ z = 0. \end{cases} \tag{16}$$

Equation (16) indicates that T(1 ∧ 5 ∧ 7 ∧ 9 ∧ 12 ∧ 13 ∧ 14 ∧ 15) is the reference configuration as shown in Fig. 9(a).

Similarly, three more transition configurations through which the 3-RER PM can switch among eight different operation modes are identified as listed in Table 7 and shown in Fig. 9(b).

Table 4
Transition configurations, T(5 ∧ j), between operation mode 5 and operation mode j($6 \le j \le 15$).

No	Constraint equations	Description
T(5 ∧ 6)	–	–
T(5 ∧ 7)	$\begin{cases} e_1 = 0 \\ e_2 = 0 \\ e_3 = 0 \\ x = 0 \\ y = 0 \end{cases}$	Configurations obtained through a translation along the Z-axis
T(5 ∧ 8)	$\begin{cases} e_0 = 0 \\ e_2 = 0 \\ e_3 = 0 \\ x = 0 \\ y = 0 \end{cases}$	Configurations obtained through a translation along the Z-axis following a half-turn rotation about the X-axis
T(5 ∧ 9)	$\begin{cases} e_1 = 0 \\ e_2 = 0 \\ e_3 = 0 \\ x = 0 \\ z = 0 \end{cases}$	Configurations obtained through a translation along the Y-axis
T(5 ∧ 10)	$\begin{cases} e_0 = 0 \\ e_2 = 0 \\ e_3 = 0 \\ x = 0 \\ z = 0 \end{cases}$	Configurations obtained through a translation along the Y-axis following a half-turn rotation about the X-axis
T(5 ∧ 11)	$\begin{cases} e_0 = 0 \\ e_2 = 0 \\ e_3 = 0 \\ x = 0 \\ y = 0 \\ z = 0 \end{cases}$	The configuration obtained through a half-turn rotation about the X-axis
T(5 ∧ 12)	$\begin{cases} e_1 = 0 \\ e_2 = 0 \\ e_3 = 0 \\ y = 0 \\ z = 0 \end{cases}$	Configurations obtained through a translation along the X-axis
T(5 ∧ 13)	$\begin{cases} e_2 = 0 \\ e_3 = 0 \\ x = 0 \\ -e_1 y + e_0 z = 0 \end{cases}$	Configurations obtained through a 2-DOF planar motion along the O–YZ plane
T(5 ∧ 14)	$\begin{cases} e_2 = 0 \\ e_3 = 0 \\ x = 0 \\ e_0 y + e_1 z = 0 \end{cases}$	Configurations obtained through a 2-DOF planar motion along the O–YZ plane
T(5 ∧ 15)	$\begin{cases} e_2 = 0 \\ e_3 = 0 \\ x = 0 \\ y = 0 \\ z = 0 \end{cases}$	Configurations obtained through a rotation about the X-axis

Table 5
Transition configurations, T(11 ∧ j), between operation mode 11 and operation mode j($12 \le j \le 15$).

No	Constraint equations	Description
T(11 ∧ 12)	$\begin{cases} e_0 = 0 \\ e_1 = 0 \\ x = 0 \\ y = 0 \\ z = 0 \end{cases}$	Configurations obtained through a rotation by $\theta_x = 2atan(e_3, e_2)$ (or $\theta_x = 2atan(-e_2, e_3)$) about the X-axis following a half-turn rotation about the Y-axis (or Z-axis)
T(11 ∧ 13)	$\begin{cases} e_0 = 0 \\ e_2 = 0 \\ x = 0 \\ y = 0 \\ z = 0 \end{cases}$	Configurations obtained through a rotation by $\theta_y = 2atan(-e_3, e_1)$ (or $\theta_y = 2atan(e_1, e_3)$) about the Y-axis following a half-turn rotation about the X-axis (or Z-axis)
T(11 ∧ 14)	$\begin{cases} e_0 = 0 \\ e_3 = 0 \\ x = 0 \\ y = 0 \\ z = 0 \end{cases}$	Configurations obtained through a rotation by $\theta_z = 2atan(e_2, e_1)$ (or $\theta_z = 2atan(-e_1, e_2)$) about the Z-axis following a half-turn rotation about the X-axis (or Y-axis)
T(11 ∧ 15)	$\begin{cases} e_0 = 0 \\ x = 0 \\ y = 0 \\ z = 0 \end{cases}$	Configurations obtained through a half-turn rotation about the axis $\mathbf{u} = \{e_1\ e_2\ e_3\}^T$

Table 6
Transition configurations, T($j \wedge 15$), between operation mode $j(1 \le j \le 14)$ and operation mode 15.

No	Constraint equations	Description
T(1 ∧ 15)	$\begin{cases} e_1 = 0 \\ e_2 = 0 \\ e_3 = 0 \\ x = 0 \\ y = 0 \\ z = 0 \end{cases}$	Reference configuration
T(2 ∧ 15)	$\begin{cases} e_0 = 0 \\ e_2 = 0 \\ e_3 = 0 \\ x = 0 \\ y = 0 \\ z = 0 \end{cases}$	Configuration obtained through a half-turn rotation about the *X*-axis
T(3 ∧ 15)	$\begin{cases} e_0 = 0 \\ e_1 = 0 \\ e_3 = 0 \\ x = 0 \\ y = 0 \\ z = 0 \end{cases}$	Configuration obtained through a half-turn rotation about the *Y*-axis
T(4 ∧ 15)	$\begin{cases} e_0 = 0 \\ e_1 = 0 \\ e_2 = 0 \\ x = 0 \\ y = 0 \\ z = 0 \end{cases}$	Configuration obtained through a half-turn rotation about the *Z*-axis
T(5 ∧ 15)	$\begin{cases} e_2 = 0 \\ e_3 = 0 \\ x = 0 \\ y = 0 \\ z = 0 \end{cases}$	Configurations obtained through a rotation about the *X*-axis
T(6 ∧ 15)	$\begin{cases} e_0 = 0 \\ e_1 = 0 \\ x = 0 \\ y = 0 \\ z = 0 \end{cases}$	Configurations obtained through a rotation about the *X*-axis following a half-turn rotation about the *Y*-axis or *Z*-axis
T(7 ∧ 15)	$\begin{cases} e_1 = 0 \\ e_3 = 0 \\ x = 0 \\ y = 0 \\ z = 0 \end{cases}$	Configurations obtained through a rotation about the *Y*-axis
T(8 ∧ 15)	$\begin{cases} e_0 = 0 \\ e_2 = 0 \\ x = 0 \\ y = 0 \\ z = 0 \end{cases}$	Configurations obtained through a rotation about the *Y*-axis following a half-turn rotation about the *X*-axis or *Z*-axis
T(9 ∧ 15)	$\begin{cases} e_1 = 0 \\ e_2 = 0 \\ x = 0 \\ y = 0 \\ z = 0 \end{cases}$	Configurations obtained through a rotation about the *Z*-axis
T(10 ∧ 15)	$\begin{cases} e_0 = 0 \\ e_3 = 0 \\ z = 0 \end{cases}$	Configurations obtained through a rotation about the *Z*-axis following a half-turn rotation about the *X*-axis or *Y*-axis
T(11 ∧ 15)	$\begin{cases} e_0 = 0 \\ x = 0 \\ y = 0 \\ z = 0 \end{cases}$	Configurations obtained through a half-turn rotation about the axis $\mathbf{u} = \{e_1\ e_2\ e_3\}^T$
T(12 ∧ 15)	$\begin{cases} e_1 = 0 \\ x = 0 \\ y = 0 \\ z = 0 \end{cases}$	Configurations obtained through a half-turn rotation about the *X*-axis followed by a half-turn rotation about the axis $\mathbf{u} = \{-e_0\ -e_3\ e_2\}^T$
T(13 ∧ 15)	$\begin{cases} e_2 = 0 \\ x = 0 \\ y = 0 \\ z = 0 \end{cases}$	Configurations obtained through a half-turn rotation about the *Y*-axis followed by a half-turn rotation about the axis $\mathbf{u} = \{e_3\ -e_0\ -e_1\}^T$
T(14 ∧ 15)	$\begin{cases} e_3 = 0 \\ x = 0 \\ y = 0 \\ z = 0 \end{cases}$	Configurations obtained through a half-turn rotation about the *Z*-axis followed by a half-turn rotation about the axis $\mathbf{u} = \{-e_2\ e_1\ -e_0\}^T$

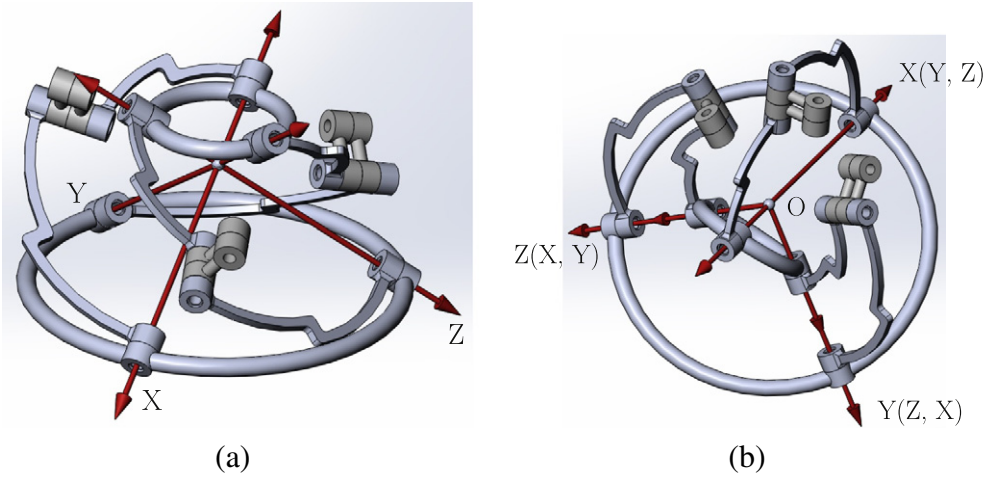

Fig. 9. Four configurations through which the 3-RER PM can switch among eight different operation modes: (a) T(1 ∧ 5 ∧ 7 ∧ 9 ∧ 12 ∧ 13 ∧ 14 ∧ 15), and (b) T(2 ∧ 5 ∧ 8 ∧ 10 ∧ 11 ∧ 13 ∧ 14 ∧ 15)(T(3 ∧ 6 ∧ 7 ∧ 10 ∧ 11 ∧ 12 ∧ 14 ∧ 15) or T(4 ∧ 6 ∧ 8 ∧ 9 ∧ 11 ∧ 12 ∧ 13 ∧ 15)).

It is noted that in the above four transition configurations of a 3-RER PM, the axes of joints 1 and 5 in each leg coincide. Each leg can rotate about the axes of joints 1 and 5. The DOF of the moving platform varies from 0 to 1 with the configuration of the legs. Therefore, the PM has 3 to 4 DOFs in total in these configurations. For a 3-RER PM with special legs in these transition configurations, the axes of joints 2 and 4 in each leg also coincide, and links 2 and 3 of a leg can rotate about the axes of joints 2 and 4. Therefore, the 3-RER PM with special legs has 6 to 7 DOFs in total in these transition configurations.

6. Conclusions

The Euler parameter quaternions have been classified into 15 cases based on the number of constant zero components and the kinematic interpretation of different cases of Euler parameter quaternions has been presented. The results have been used to the reconfiguration analysis of a 3-DOF 3-RER parallel mechanism with orthogonal platforms. It has been found that the parallel mechanism has 15 3-DOF operation modes, including one spherical mode, four translational modes, six planar modes and four zero-torsion-rate motion modes. The transition configurations among different operation modes have been obtained. Four

Table 7
Transition configurations in which the 3-RER parallel mechanism can switch among eight operation modes.

No	Type	Constraint equations	Description
1	T(1 ∧ 5 ∧ 7 ∧ 9 ∧ 12 ∧ 13 ∧ 14 ∧ 15)	$\begin{cases} e_1 = 0 \\ e_2 = 0 \\ e_3 = 0 \\ x = 0 \\ y = 0 \\ z = 0 \end{cases}$	Reference configuration (Fig. 9 (a))
2	T(2 ∧ 5 ∧ 8 ∧ 10 ∧ 11 ∧ 13 ∧ 14 ∧ 15)	$\begin{cases} e_0 = 0 \\ e_2 = 0 \\ e_3 = 0 \\ x = 0 \\ y = 0 \\ z = 0 \end{cases}$	Configuration obtained through a half-turn rotation about the *X*-axis (Fig. 9 (b))
3	T(3 ∧ 6 ∧ 7 ∧ 10 ∧ 11 ∧ 12 ∧ 14 ∧ 15)	$\begin{cases} e_0 = 0 \\ e_1 = 0 \\ e_3 = 0 \\ x = 0 \\ y = 0 \\ z = 0 \end{cases}$	Configuration obtained through a half-turn rotation about the *Y*-axis (Fig. 9 (b))
4	T(4 ∧ 6 ∧ 8 ∧ 9 ∧ 11 ∧ 12 ∧ 13 ∧ 15)	$\begin{cases} e_0 = 0 \\ e_1 = 0 \\ e_2 = 0 \\ x = 0 \\ y = 0 \\ z = 0 \end{cases}$	Configuration obtained through a half-turn rotation about the *Z*-axis (Fig. 9 (b))

transition configurations have also been identified in which the parallel mechanism can switch among 8 operation modes. To the best knowledge of the author of this paper, this is the first report on the finding that a parallel mechanism can switch among 8 operation modes in a transition configuration.

Although the 3-RER parallel mechanism with orthogonal platforms is not of practical industrial use due to the limited workspace in each operation mode, it is valuable for teaching robot kinematics since this PM covers four different types of 3-DOF motion and can also be used to demonstrate concepts of constraint singularity and kinematic singularity in different operation modes. A prototype has been fabricated and used in teaching robot kinematics at Heriot-Watt University.

The classification and kinematic interpretation of Euler parameter quaternions presented in this paper may help further promote the application of Euler parameter quaternions in the analysis and design of parallel mechanisms, especially parallel mechanisms with multiple operation modes.

Acknowledgments

The author would like to thank the Engineering and Physical Sciences Research Council (EPSRC), United Kingdom, for supporting this work under grant No. EP/I016333/1.

References

[1] X. Kong, C. Gosselin, P.L. Richard, Type synthesis of parallel mechanisms with multiple operation modes, ASME J. Mech. Des. 129 (6) (2007) 595–601.
[2] X. Kong, Type synthesis of 3-DOF parallel manipulators with both a planar operation mode and a spatial translational operation mode, ASME J. Mech. Robot. 5 (4) (2013) 041015.
[3] P. Fanghella, C. Galleti, E. Gianotti, Parallel robots that change their group of motion, in: J. Lenarčič, B. Roth (Eds.), Advances in Robot Kinematics, Springer, The Netherlands, 2006, pp. 49–56.
[4] S. Refaat, J.M. Hervé, S. Nahavandi, H. Trinh, Two-mode overconstrained three-DOFs rotational-translational linear-motor-based parallel kinematics, mechanism for machine tool applications, Robotica 25 (2007) 461–466.
[5] Q. Li, J.M. Hervé, Parallel mechanisms with bifurcation of Schoenflies motion, IEEE Trans. Robot. 25 (1) (2009) 158–164.
[6] G. Gogu, Maximally regular T2R1-type parallel manipulators with bifurcated spatial motion, ASME J. Mech. Robot. 3 (1) (2011) 011010.
[7] K.H. Hunt, Kinematic Geometry of Mechanisms, Cambridge University Press, Cambridge, 1978.
[8] D. Zlatanov, I.A. Bonev, C.M. Gosselin, Constraint singularities as C-Space singularities, in: J. Lenarčič, F. Thomas (Eds.), Advances in Robot Kinematics—Theory and Applications, Kluwer Academic Publishers, 2002, pp. 183–192.
[9] D. Gan, J.S. Dai, Q. Liao, Mobility change in two types of metamorphic parallel mechanisms, ASME J. Mech. Robot. 1 (4) (2009) 041007.
[10] D.A. Cox, J.B. Little, D. O'Shea, Ideals, Varieties, and Algorithms, Springer, 2007.
[11] D.R. Walter, M.L. Husty, M. Pfurner, Chapter A: complete kinematic analysis of the SNU 3-UPU parallel manipulator, Contemporary Mathematics, American Mathematical Society, Vol 496, 2009, pp. 331–346.
[12] A.J. Sommese, C.W. Wampler II, The Numerical Solution of Systems of Polynomials Arising in Engineering and Science, World Scientific, 2005.
[13] W. Decker, G. Pfister, A First Course in Computational Algebraic Geometry Cambridge University Press, 2013.
[14] K.W. Spring, Euler parameters and the use of quaternion algebra in the manipulation of finite rotations: a review, Mech. Mach. Theory 21 (5) (1986) 365–373.
[15] W.F. Phillips, C.E. Hailey, Review of attitude representations used for aircraft kinematics, J. Aircr. 38 (4) (2001) 718–737.
[16] I. Bonev, Geometric Analysis of Parallel Mechanisms, PhD Thesis Laval University, Quebec, Canada, 2002.